

S. C. BLANK,  
College of Aeronautics,  
Cranfield University,  
Cranfield, Bedford, UK.

## Abstract

Experiments were performed at a nominal Mach number of 2.5 and Reynolds numbers ( $Re_\delta$ ) of  $4.1 \times 10^4$  and  $6 \times 10^4$  in order to investigate the effects of the glancing shock wave / turbulent boundary layer interaction produced by a series of hemi-cylindrically blunted fins mounted individually on a flat plate. Strakes were added to the fin / flat plate junction in an attempt to modify the interaction's strength. Mean static pressures measurements on the side wall, surface oil flow pictures taken over the side wall and the fin, and schlieren pictures taken in two planes normal to each other were the main data collection methods. It was found that the strakes attenuated the undesirable features of the flow field.

## Introduction

A significant amount of research effort has been concentrated on investigating the characteristics of the flow field around supersonic wing - body junctions. The wing's bow shock wave impinges upon the fuselage's turbulent boundary layer (fig. 1) and this creates many problems for the aircraft designer. Firstly, the adverse pressure gradients generated in the subsonic section of the boundary layer cause the flow to separate. Within the separated region a number of vortices are formed and the number of vortices depends upon the Reynolds number of the flow (1) & (2). Secondly, an Edney type IV shock / shock interaction is created because the bow shock wave bifurcates close to the wing root (3). Very high heat peaks have been recorded as a result of such interactions. The third obstacle in the designer's path is the high static pressures created around the junction. Pressure peaks six times the freestream pressure are not unknown. Finally, flow field unsteadiness introduces an additional complication.

Most of the research conducted until the early 1990's concentrated on understanding the features of the flow field or investigating the effects of suction / blowing on the interaction. Only a few researchers have considered passive methods of alleviating the interaction and milestone contributions in this field have been forthcoming from Blank (4), Lakshmanan et al (5), Koide and Stollery (6) and Haq (7).

Lakshmanan et al's computational study indicated that significant improvements in the pressure distribution occurred when a fillet of 3.5 times the leading edge diameter (D) was used. Unfortunately, at the time of writing there was no experimental data against which they could compare their results for filleted fins. Haq (8) used a configuration identical to Lakshmanan et al's and his experimental results compare favourably with Lakshmanan et al's. However, Haq did not take any pressure

measurements so one is still unable to validate all of Lakshmanan et al's work.

The author (4) produced one of the first sets of supersonic experimental data for blunt fins with fillets and Koide and Stollery (6) followed shortly afterwards with data for sharp fins. Blank (4) investigated the effects of triangular ramp type fillets and his flow visualisation experiments indicated that the fillets did not appear to improve the interaction. Koide and Stollery found similar results for their small fillet placed around a sharp fin.

The current research programme is aimed at illustrating the effects of incorporating strakes into a straight wing / body junction at supersonic speeds. The aims of the project were to reduce :

- the pressure levels experienced ahead of and around the junction,
- the area of separated flow generated by the junction and,
- the unsteadiness of the shock system.

## Experimental Detail

The experiments detailed within this paper were conducted in two facilities namely, the College of Aeronautics' continuous 9" x 9" and intermittent 2.5" x 2.5" supersonic wind tunnels. Details of the freestreams' properties can be found in Table 1. Both facilities had fully developed turbulent boundary layers growing under zero pressure gradients along the working section walls. All the tests were conducted with the fins at zero degrees of incidence.

The following configurations were examined in the 9" x 9" wind tunnel (see fig. 2 Sections A and B):

- (1) an unmodified straight fin of  $D/\delta=1.6$ ,
- (2) a sharp leading edge strake attached to (1),
- (3) an unmodified straight fin of  $D/\delta=0.6$ , and,

<sup>1</sup> This paper serves as an update to the work presented at the 18th ICAS Congress (see ICAS 92-7.9.2).

- (4) a blunt leading edge strake of height (h) to  $\delta$  ratio of 1.6 attached to configuration (3).

In order to investigate the effects of the height of a blunt leading edge strake the following configurations of  $D/\delta=0.682$  were considered in the 2.5" x 2.5" wind tunnel (see fig. 2 Section C):

- (5) a 45° swept fin of height (h) to  $\delta$  ratio of 1.6,  
(6) configuration (5) attached to a straight fin of the same  $D/\delta$  ratio,  
(7) a 45° swept fin of height (h) to  $\delta$  ratio of 3.2,  
(8) configuration (7) attached to a straight fin of the same  $D/\delta$  ratio,

All of the techniques used to obtain the data presented in this paper are described in ref. 4 except for the high speed photography system. This system was similar to the single pass schlieren system described in ref. 4 except for a Hadland Hyspeed cine camera (set to 4,000 frames / second and loaded with Kodak RAR 2479 400 ASA film) replacing the Olympus camera and a 650 W tungsten filament bulb instead of the 1  $\mu$ s spark source.

## Results and Discussion

### A) Sharp Leading Edge Strakes (Cases 1 & 3)

Some indication of the complexity of the basic flow field can be grasped by examining fig. 3 (a). This figure implies that the four vortex model proposed by Sedney and Kitchens<sup>(2)</sup> is applicable to the present fin. The oil flow pattern for the sharp strake indicates that the part of the flow near the strake's leading edge root is characteristic of normal swept sharp fin flow (fig. 3 (b)). This region of flow, bounded by the incomplete separation lines either side of the strake, will be termed "strake dominated". Clearly, the vast majority of the flow field is similar to the flow field generated by the unmodified fin of  $D/\delta=1.6$  so this region of flow will be termed "fin dominated". The strake has a local effect on the location of the primary separation line as the onset of separation is delayed in the vicinity of the fin's centre line by about 0.2 to 0.4 D.

The pressure data (fig. 4) reveals that the strake significantly alters the pressure distribution close to the fin. Firstly, the strake delays the pressure rise. Secondly, the pressure peaks for the modified fin are lower than the corresponding peak pressures for the unmodified fin and thirdly, the relationship between the location of the separation and attachment lines to regions of falling and rising pressure has been altered by the introduction of the sharp strake.

At  $Y=0.75$ " (fig. 4 (b)) the height of the second peak generated by the modified fin is about 30% lower than the corresponding peak for the unmodified fin. Note also, that the adverse pressure gradient between  $S_2$  and  $A_2$  is significantly lower than that experienced by the unmodified fin. These two effects of the strake have resulted in the

formation of a region, around D in length, of slightly adverse pressure gradient. These effects suggest that the strake has had a significant effect upon the vortical nature of the flow close to the fin and that it has reduced the relative amount of reversed flow between  $A_2$  and  $A_1$ .

Normally, flow separates when it encounters an adverse pressure gradient and thus, when  $S_2$  is located in a region of decreasing pressure it is indicative of the majority of the flow local to  $S_2$  being reversed. The change in the location of  $S_2$  that the strake has caused implies that the strake has reduced the amount of reversed flow relative to flow in the freestream direction about  $S_2$ .

By  $Y = 1.75$ " the pressure plots for the two flow fields start to resemble each other. This indicates that the effects of the strake on the pressure field are becoming muted and the influence of the unmodified fin is becoming dominant.

From the results of these experiments it is believed that the key to designing a successful strake is the balancing of the favourable effects of the strake against the adverse pressure gradient produced by the fin's bluntness. Thus, the strake's sweep angle ( $\lambda_s$ ), height (h) and bluntness ( $D_s$ ) are the fundamental design parameters for diminishing the adverse pressure gradient generated by the unmodified configuration.

### B) Blunt Leading Edge Strakes

In this section the flow fields produced by the models in Sections B & C of fig. 2 will be compared. The models in Section B of fig. 2 were tested in the 9" x 9" wind tunnel whilst those in Section C were examined in the smaller wind tunnel.

#### (i) The Models of $D/\delta=0.6$ (Cases 4 & 5)

Oil flow photographs for these two models are displayed in fig. 5. They clearly show how the addition of the strake to the leading edge has altered the flow field. The separation line pattern around the root of the strake (fig. 5 (b)) suggests that there are 4 horseshoe vortices consisting of two contra-rotating pairs. Further downstream, the influence of the unswept part of the fin on the flow field is felt as a third separation and attachment line pair is present,  $S_3$  &  $A_3$  (fig. 5 (b)). In the lower half of the fig. 5 (b)  $S_1$  and  $S_3$  converge and eventually run almost parallel to each other.

Schlieren images of the shock structures produced by the models (fig. 6) clearly illustrate that the strake generates its own detached bow shock, herein termed the "strake shock". This shock wave interacts with the fin's bow shock to create an Edney type IV shock / shock interaction. Based upon analysis of a high speed cine film the strake shock is significantly more stable than the separation shock wave produced by the unmodified fin. The length scale of the motion of the separation shock was determined to be 1.25D against 0.5D for the strake shock. In addition, the length scale of the triple point's vertical motion was found

to reduce from  $0.27\delta$  to  $0.13\delta$  upon the introduction of the strake.

The strake shock appears to oscillate only up to a height of  $1.3\delta$  above the fin / wall interface and the section of the strake-shock between  $1.3\delta$  and the triple point is virtually motionless. Occasionally, small fluctuations of the triple point occur and these are usually the result of the foot of the strake shock undergoing a larger than normal motion which does not become fully damped before reaching the triple point. Also, it was found that the length scale of the strake shock's motion (when expressed in terms of  $D$ ) correlates to the length scale of the separation shock's motion for a "semi-infinite" fin of the same sweep angle as the strake.

The blunt strake is an excellent method for reducing the peak pressures experienced around a straight blunt fin (fig. 7). Indeed, at  $Y=0.25$ " the peak pressure has been reduced by a factor of 50% and this trend of reducing the peak pressure continues until  $2D$  ( $Y=0.75$ "") outboard of the fin's centreline. Beyond  $Y=0.75$ " the strake does not produce any reduction in peak pressure. It is interesting to note that up to  $Y=0.75$ " the strake has substituted two small pressure peaks for the large peak generated by the unmodified fin.

If the location of the separation and attachment lines are superimposed upon the pressure plots it is found that the two small pressure peaks generated by the modified model correspond to the pressure rises induced by the strake and the straight portion of the leading edge. Note how the pressure peak generated by the strake reduces as  $Y$  is increased.

Between  $Y=0.25$  and  $0.75$ " the separation lines for the modified fin are located in regions of rising pressure (based on the freestream direction). Secondary separation for the unmodified fin usually resides in a region of falling pressure which implies that the majority of the flow local to  $S_2$  in the unmodified case is reversed. However, as all of the separation lines for the modified fin are in regions of rising pressure the strake has caused the relative amount of the flow passing  $S_2$  in the freestream direction to become greater than the amount of flow in the opposite direction.

When considered together the oil flow photographs and the pressure data suggest that the flow re-attaches to the wall at  $A_2$  and separates further downstream at  $S_3$ . At  $S_3$  the flow rolls-up to form the vortex  $V_5$  as illustrated in the flow field model in fig. 8 (b).

The distance between the separation lines  $S_1$  and  $S_3$  appears to be dependent upon  $Y$  (fig. 5 (b) & 8 (b)). When  $Y$  is small the distance between  $S_1$  and  $S_3$  is relatively large, but as  $Y$  is increased this distance decreases until they run almost parallel. Prior to  $S_1$  and  $S_3$  running almost parallel to each other, the separation line  $S_2$  appears to merge with  $S_3$  leaving only  $S_1$  and  $S_3$  (figs. 5 (b) & 8 (b)). The implications of this are that  $V_3$  and  $V_4$  either dissipate or merge with the other vortices. Thus,  $V_1$ ,  $V_2$ ,  $V_5$  and  $V_6$  prevail but the distance between  $V_1$  and  $V_5$  is significantly less than that prior to the merger. The vortices  $V_1$  and  $V_2$  are weaker than  $V_5$  (see fig. 8 (b) then compare fig. 7 (f) & (h)) and therefore the latter dominates

in the far field region. The reason behind the dominance of  $V_5$  is that  $V_1$  to  $V_4$  are generated through the interaction of the strake on the flow field and that  $V_5$  is the result of the blunt fin's influence on the flow. The adverse pressure gradient generated by the strake when assessed independently, is smaller than that created by the fin alone due to the effects of leading edge sweep and therefore, the pressure gradients that the different components of the wing create have different strengths.

The blunt strake has had a net positive effect on the flow field with respect to the programme's aims and the concept of using a blunt strake to attenuate the undesirable flow features of a wing / body junction is an excellent way to obtain the benefits of leading edge sweep without sacrificing the surface area of a control surface.

#### (ii). The Models of $D/\delta=0.682$ (Cases 5 to 8)

The four models illustrated in Section C of fig. 2 were used to investigate (1) the effects of the height of the strake when used independently and (2) how increasing the height of the strake when attached to the straight portion of the wing influences the flow on the wall. Two of the models consist of the basic strake (termed "strake only") and the other two models incorporate the strake and the straight outer portion of the wing. All of the models were of a  $D/\delta$  ratio slightly above that used in the 9" x 9" wind tunnel because earlier work had indicated that a smaller width fin would encounter severe mounting problems.

The first two models had identical  $h/\delta$  and  $\lambda_s$  values to the earlier blunt strake model. A sketch of the plan view oil flow photograph for the bare strake (fig. 9 (a)) indicates the presence of three distinct separation lines. The first two of which,  $S_1$  and  $S_2$ , are located in a horseshoe manner around the leading edge of the fin whilst the third separation line leaves the shoulder of the model at a slight angle until it is deflected outwards. This outward movement of  $S_3$  appears to be caused by the mounting arrangement used to hold the model in place because a comparison of the streamline patterns for the series of  $45^\circ$  hemi-cylindrically blunted fins tested by Hussain<sup>(9)</sup> do not indicate the existence of any similar effects on  $S_3$ .

However, when the straight fin is added to the strake the oil flow photograph for this model, fig. 9 (b), suggests that the flow field for this model is qualitatively similar to that generated by the Case 4 blunt strake model (fig. 5 (b)). The location of the primary separation line,  $S_1$ , until it approaches  $S_4$  is identical to the position of the primary separation line generated by the corresponding "strake only" model (Case 5) in fig. 9 (a). This implies that there is a region of flow within the modified fin's flow field which assumes the characteristics of the flow field generated by the strake.

The qualitative character of the oil flow patterns on the wall do not appear to have been affected by the 27% change in  $Re_\delta$  or the 20% variation in  $H$  nor the 12% alteration in  $D/\delta$  between the Case 4 and the Case 6 (see Table 2). Indeed the  $L/\delta$  value for this fin is 1.3 which is identical to the value for Case 4. As both  $D_s/\delta$  and  $D/\delta$  were

altered simultaneously the beneficial effects of an increase in  $D_s/\delta$  were probably negated by the increase in  $D/\delta$ . Hence, we can conclude that the increase in  $Re_\delta$  from  $41.6 \times 10^3$  to  $57.3 \times 10^3$  and the increase in  $H$  from 3.75 to 4.66 did not affect  $L/\delta$  in any perceivable manner.

Two pairs of separation,  $S_1$  &  $S_2$ , and attachment,  $A_1$  &  $A_2$ , lines are identifiable in the oil flow pattern produced by the Case 7 model (fig. 9 (c)). The separation and attachment line pattern produced by this model suggests that the flow rolls-up to form a number of horseshoe vortices around the leading edge of the wing in a manner similar to that for the Case 5 model above. The location of  $S_1$  for both of the "strake only" models (Cases 5 & 7) are identical. This implies that the increase in strake height has not affected the location of the primary separation line. No change in the location of the separation line was expected because the majority of the shock wave for the  $h/\delta = 1.6$  model is located where the inviscid shock wave would be located. Thus, any increase in the strake's height, above  $h/\delta = 1.6$ , does not affect what happens at the root of the strake.

A number of important effects occurred when the straight portion of the wing was added to the Case 7 model. Firstly, the change in  $h/\delta$  between Cases 6 and 8 has caused the region of fin dominated flow to decrease dramatically. The location of the primary separation line,  $S_1$ , (fig. 9 (d)) coincides with the location of the primary separation line,  $S_1$ , generated by the Case 7 model (fig. 9 (c)) until slightly upstream of the trailing edge. Secondly, note that unlike Cases 4 & 6, the secondary separation line deviates from the position of the secondary separation line produced by the independent strake prior to any deviation in the path of the primary separation line. This may have occurred, because the strake dominates a far greater quantity of the flow than in Cases 4 & 6 and as a result of this, the primary separation line is located too far outboard of the fin to enable the primary separation line to be influenced first (see Region A in fig. 9 (d)).

Thirdly, there is no separation line that can be deemed to be the equivalent to  $S_3$  in Cases 4 & 6. In the present example, the fin's influence on the flow field is merely the deviation of the separation lines  $S_1$  &  $S_2$ . The straight portion of the leading edge first influences the flow field at  $4.2\delta$  downstream of the leading edge. Table 2 indicates that the only parameter that has been changed between Case 6 and Case 8 is  $h/\delta$ . Furthermore, Table 2 shows that a 100% change in  $h/\delta$  caused a change in  $L/\delta$  in excess of 300% when all the other parameters remained constant. It can be stated therefore, that  $L/\delta$  is not dependent upon  $h/\delta$  through a first order relationship such as  $\left(\frac{L}{\delta}\right) = A\left(\frac{h}{\delta}\right)$ , where  $A = \text{a constant}$ .

During the experimental programme the following parameters were altered :  $D/\delta$ ,  $h/\delta$ ,  $M$ , and  $Re_\delta$ . Hence, we can state that  $L/\delta$  is some function of the parameter set  $\left\{\frac{D}{\delta}, M, Re_\delta, \frac{h}{\delta}\right\}$  when  $D/\delta = D_s/\delta$  and  $\lambda_s$  remains constant.

Kleifges (9) recently conducted tests on a similar blunt strake configuration and his data are included in Table 2 along with the present programme's data. A large number of parameters have been altered between Kleifges' experiment and the current experiments. This does not aid the identification of the variables controlling  $L/\delta$  and a "back to basics" approach has to be adopted due to the meagre size of the database available.

Below is the author's hypotheses with regards to various parameters influence on the  $L/\delta$  values produced by models such as Case 4 in fig. 2. The following statements relate to changes in *geometric* parameters *not* flow properties except where mentioned. Furthermore, the parameters under discussion is considered to be altered in isolation, and all the other parameters remain constant.

(a)  $D/\delta$ . An increase in  $D/\delta$  is expected to result in an upstream movement of the location of the fin's influence on the flow field and vice versa (see refs. 7 & 11). Hence,  $L/\delta$  will decrease as  $D/\delta$  increases.

(b)  $D_s/\delta$ . A decrease in  $D_s/\delta$  will cause a reduction in the strength of the strake shock. Hence, the amount of strake dominated flow will reduce and  $L/\delta$  will decrease.

(c)  $h/\delta$ . The available data indicates that the strake has to be a multiple of  $\delta$  in order to be effective (e.g.  $h \geq 1.4\delta$ ). From Table 2 it appears that  $h/\delta$  strongly influences  $L/\delta$  and  $\epsilon$  (see fig. 10). The  $\epsilon$  value for Kleifges data corresponds to those for Cases 4 & 6 and this issue warrants further study. Interestingly, all of the propagation angles are greater than their corresponding Mach angles and this implies that the disturbance is dependent upon the subsonic flow's properties.

(d)  $\lambda_s$ . Strakes with little or no sweep are unlikely to affect the flow field as their pressure fields will almost match the unmodified fin's. Fins with high sweep angles (8) do not cause significant effects upon the flow field when they are inserted into flow field independently. Thus, the sweep of the strake has to be moderate and between the two extremes. In addition, the height of the strake has to be considered so note the remarks in (c) above. Based upon the results for swept fins produced by Hussain (8) it is believed that the strake would require between  $30^\circ$  and  $60^\circ$  of sweep (and  $h > \delta$ ) if significant mitigation effects in vortex strength are desired.

(e) Mach number. The stand-off distance of the bow shock wave around a circular cylinder decreases as Mach number is increased (12). Hence, it is expected that the most upstream point of the fin's influence on the flow field would move downstream in a similar manner to that for the location of the bow shock wave. This would result in an increase in the propagation angle,  $\epsilon$  (see fig. 10) and  $L/\delta$ .

## Conclusions

Experiments have been conducted to investigate the effect of introducing strakes into unswept fin / fuselage junctions at supersonic speeds. Significant flow field changes have resulted and are summarised below.

### A. Sharp Leading Edge Strakes

The incorporation of a sharp leading edge strake into the wing / fuselage junction resulted in the creation of two regions of flow ("strake" and "fin" dominated) in which the different components of the wing dominated the flow field structure.

### B. Blunt Leading Edge Strakes

When a blunt leading edge strake was incorporated into the junction it affected the flow field such that :

- there are regions of both "strake" and "fin" dominated flow and the flow in each of these regions mirrors the flow field generated by the components of the wing when used independently,
- the unsteadiness of the flow field was significantly reduced, and,
- a net decrease in the pressure levels experienced around the fin and in the area of separated flow occurred.

### Acknowledgements

The author is indebted to his supervisor Prof. J. L. Stollery and the College's technical staff for their constant help and advice.

### References

1. *Stollery, J. L.*, 1989, "Glancing Shock - Boundary Layer Interactions", AGARD Report No. 764 - Special Course on Three-Dimensional Supersonic / Hypersonic Flows Including Separation. FDP/VKI/ CPP.
2. *Sedney, R., and Kitchens, C. W.*, 1977, "Separation Ahead of Blunt Protuberances in Supersonic Turbulent Boundary Layers", AIAA J., Vol. 15, No. 4, pp. 546-552, April 1977.
3. *Edney, B.*, 1968, "Anomalous Heat-Transfer and Pressure Distributions on Blunt Bodies at Hypersonic Speeds in the Presence of an Impinging Shock", FFA Report no. 115.
4. *Blank, S. C.*, 1992, "Supersonic Wing Body Interference", ICAS 92-7.9.2.
5. *Lakshmanan, B., Tiwari, S. N. and Hussaini, M. Y.*, 1988, "Control of Supersonic Interaction Flow Fields Through Filleting and Sweep", AIAA/ASME/SIAM/APS First National Fluid Dynamics Congress, July 1988.
6. *Koide, S. and Stollery, J. L.*, 1993, "Effects of Junction Modifications on Sharp Fin Induced Shock Wave / Boundary Layer Interaction", AIAA 93-2935.
7. *Hag, Z. U.*, 1993, "Hypersonic Vehicle Interference Heating", PhD Thesis, Department of Aeronautics and Astronautics, University of Southampton, August 1993.
8. *Fomison, N. R.*, 1986, "The Effects of Bluntness and Sweep on Glancing Shock Wave Turbulent Boundary Layer Interaction" PhD Thesis, College of Aeronautics, Cranfield Institute of Technology. See also *Fomison, N. R. and Stollery, J. L.*, 1987, "The Effects of Sweep and Bluntness on a Glancing Shock Wave Turbulent Boundary Interaction", AGARD CP 423.
9. *Hussain, S.*, 1985, "A Study of the Interaction Between a Glancing Shock Wave and a Turbulent Boundary Layer - The Effects of Leading

Edge Bluntness and Sweep", PhD Thesis, College of Aeronautics, Cranfield Institute of Technology, November 1985.

10. *Kleifges, K.*, 1993, "An Experimental Investigation of the Effects of Leading Edge Geometry on the Dynamics of Blunt Fin-Induced Shock Wave Turbulent Boundary Layer Interaction", MSE Thesis, The University of Texas at Austin, May 1993.
11. *Blank, S. C.*, "Passive Techniques of Controlling Flow in Supersonic Wing / Body Junctions", PhD Thesis, College of Aeronautics, Cranfield Institute of Technology, To be published.
12. *Saida, N., and Hattori, H.*, 1984, "Shock Wave-Turbulent Boundary Layer Interactions Induced by a Blunt Fin", Transactions of the Japan Society for Aeronautical and Space Sciences, Vol. 27, No. 76.
13. *Liepmann, H. W., and Roshko, A.*, 1957, "Elements of Gas Dynamics", John Wiley & Sons Inc.

**Table 1. Freestream Properties in the Wind Tunnels and Notation**

#### (a) Freestream Properties in the Wind Tunnels

Property	Wind Tunnel	
	9" x 9"	2.5" x 2.5"
Mach Number, M.	2.45	2.43
Reynolds Number, $Re_\delta$ ( $\times 10^3$ )	41	59.6
Stagnation Pressure, $P_{01}$ (kPa)	24.8	100.4
Stagnation Temperature, $T_{01}$ (K)	293	293
Boundary Layer Thickness (99.5%), $\delta$ (inches)	0.625	0.23
Boundary Layer Displacement Thickness, $\delta^*$ (inches)	0.14	0.07
Boundary Layer Momentum Thickness, $\theta$ (inches)	0.04	0.0015

#### (b) Other Notation

Symbol	Definition	Units
A	Attachment line	
D	Body diameter (subscript "s" denotes strake)	inches
H	Boundary layer shape parameter	
S	Separation line	
T	Turn-table / tunnel wall interface	
U	Upstream influence line	
X	Longitudinal distance from the model's leading edge	inches
Y	Lateral distance from the model's centre line	inches
h	Height of the strake	inches
$\delta$ or delta	Boundary layer thickness (99.5%)	inches
$\epsilon$	Angle which the fin's influence on the flow field propagates	degrees
$\lambda$	Leading edge sweep (subscript "s" denotes strake)	degrees
$\mu$	Mach angle	degrees

**Table 2. Data Table for the Strake / Fin Combinations**

Case No.	D/ $\delta$	h/ $\delta$	L/ $\delta$	M	$Re_\delta$ $10^3$	H	$\epsilon$ deg.	$\mu$ deg.
2	1.6	1.6	-1.9	2.45	41.6	3.75	N/A <sup>1</sup>	N/A
4	0.6	1.6	1.3	2.45	41.6	3.75	51	22
6	0.682	1.6	1.3	2.43	57.3	4.667	51	22
8	0.682	3.2	4.2	2.43	57.3	4.667	37	22
Kleifges	1.27	1.4	1.14	4.95	717	10	51	11

<sup>1</sup> N/A = Not Applicable.

**Fig. 1. Schematic Diagram of the Flow Field.**

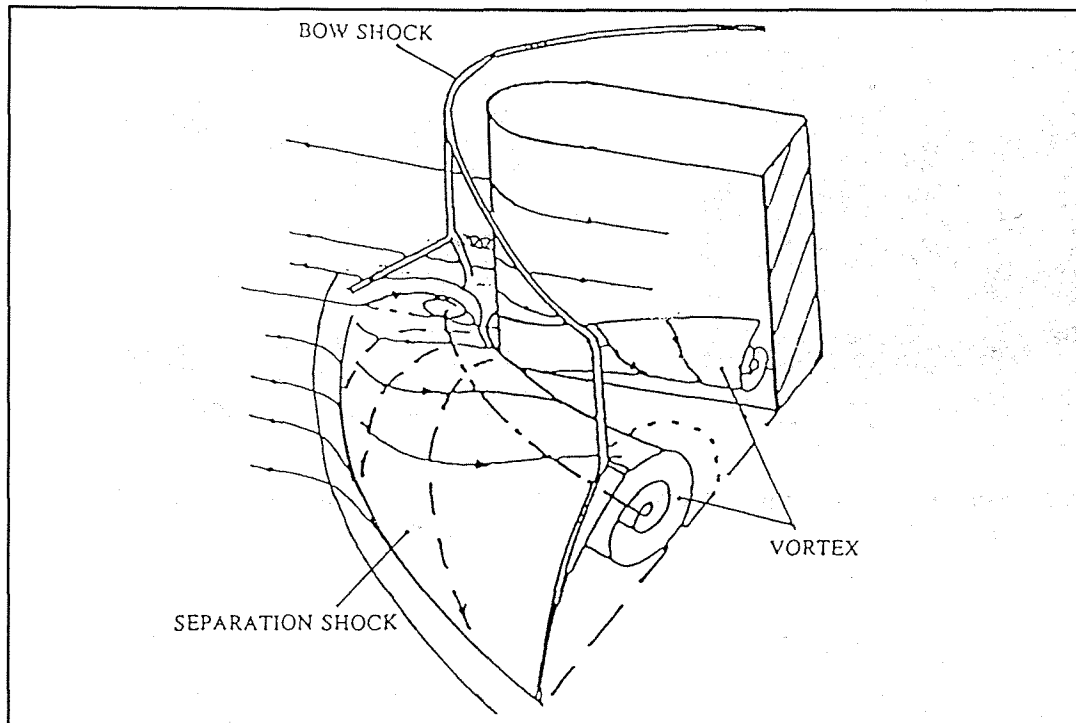


**Fig. 2. Details of the Models Used During the Experimental Programme**

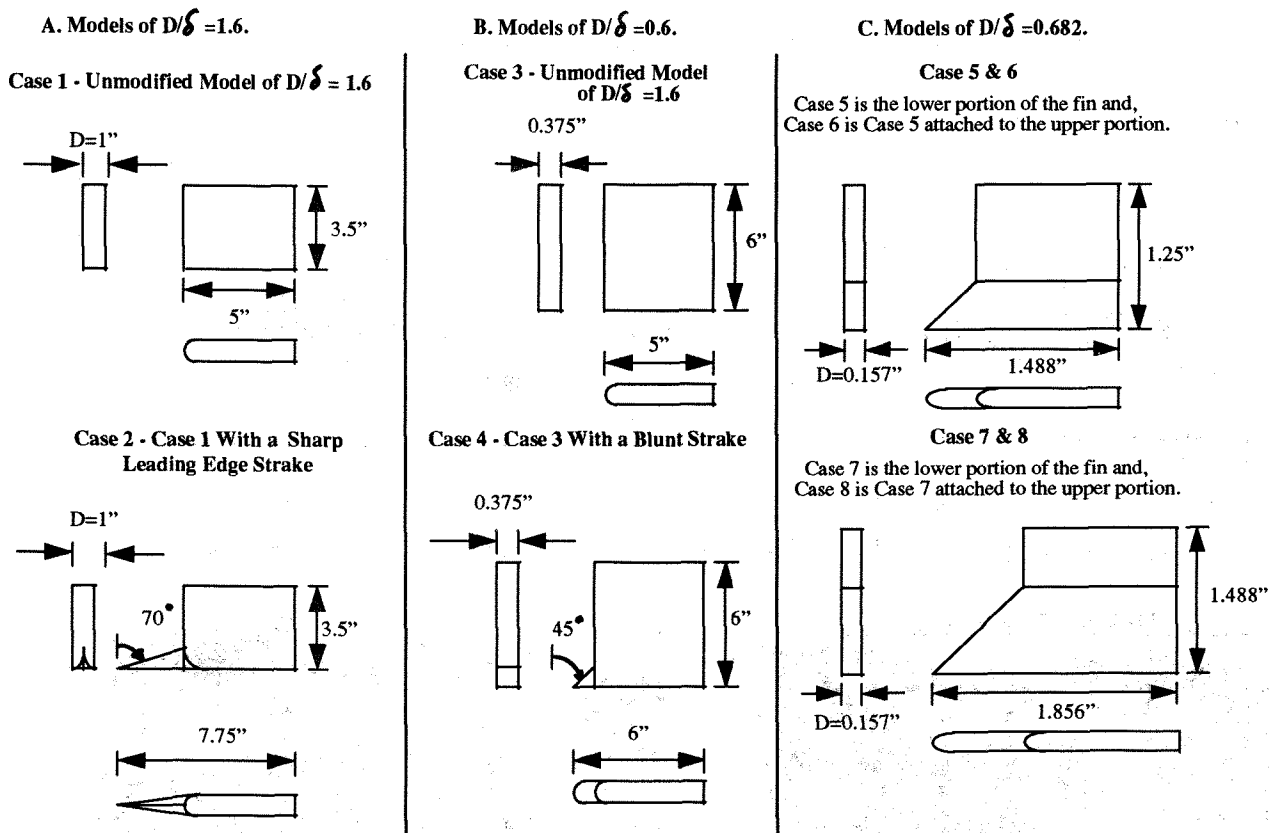


Fig. 3. Oil Flow Photographs for the  $D/\delta=1.6$  and its Derivatives

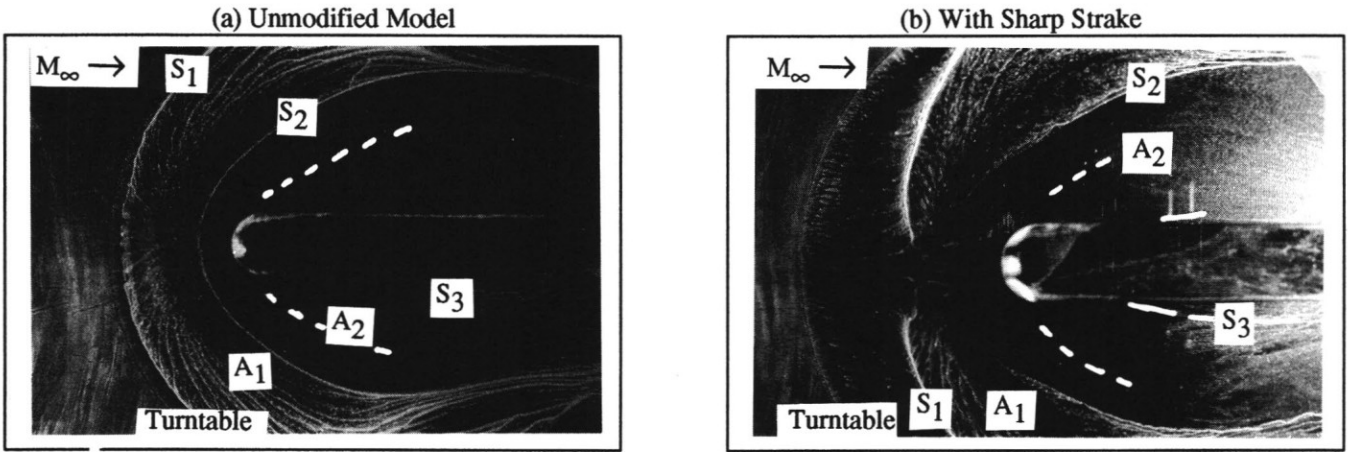


Fig. 4. Pressures for the  $D/\delta=1.6$  Model With and Without a Sharp Leading Edge Strake

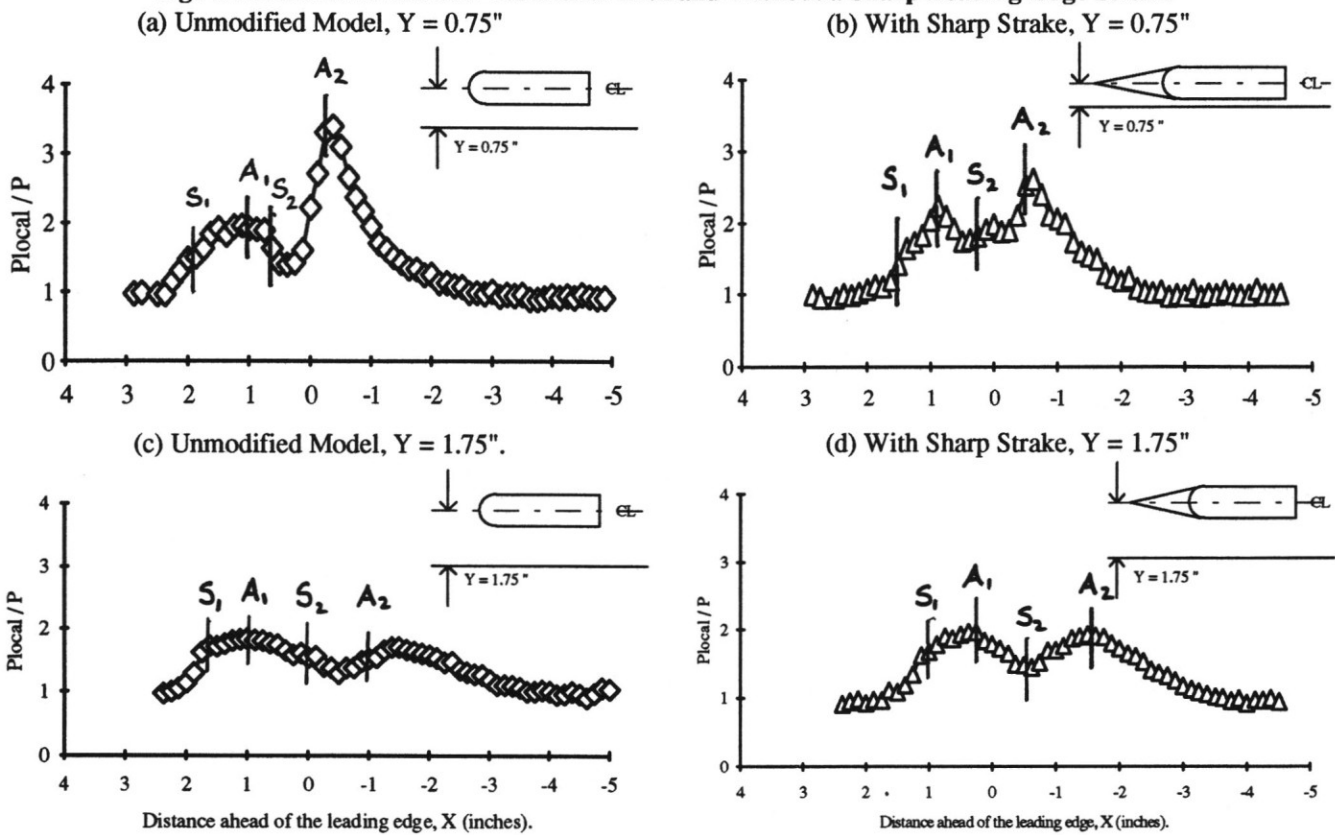
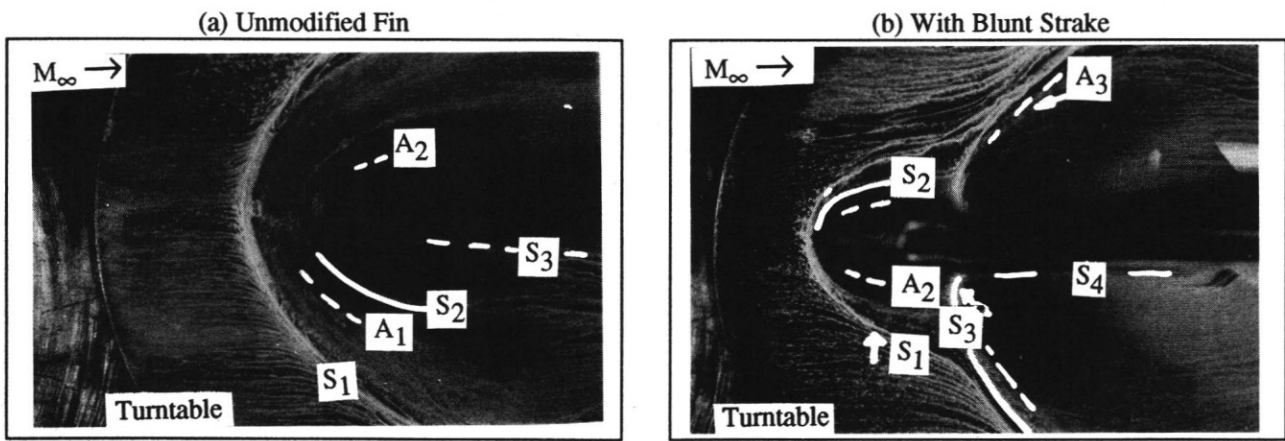
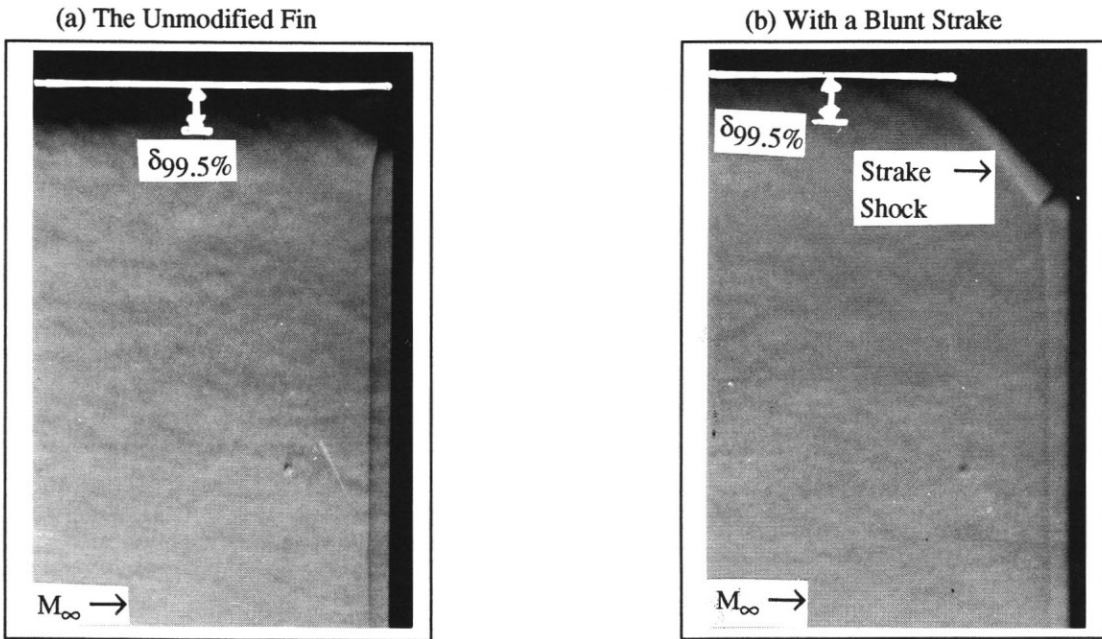


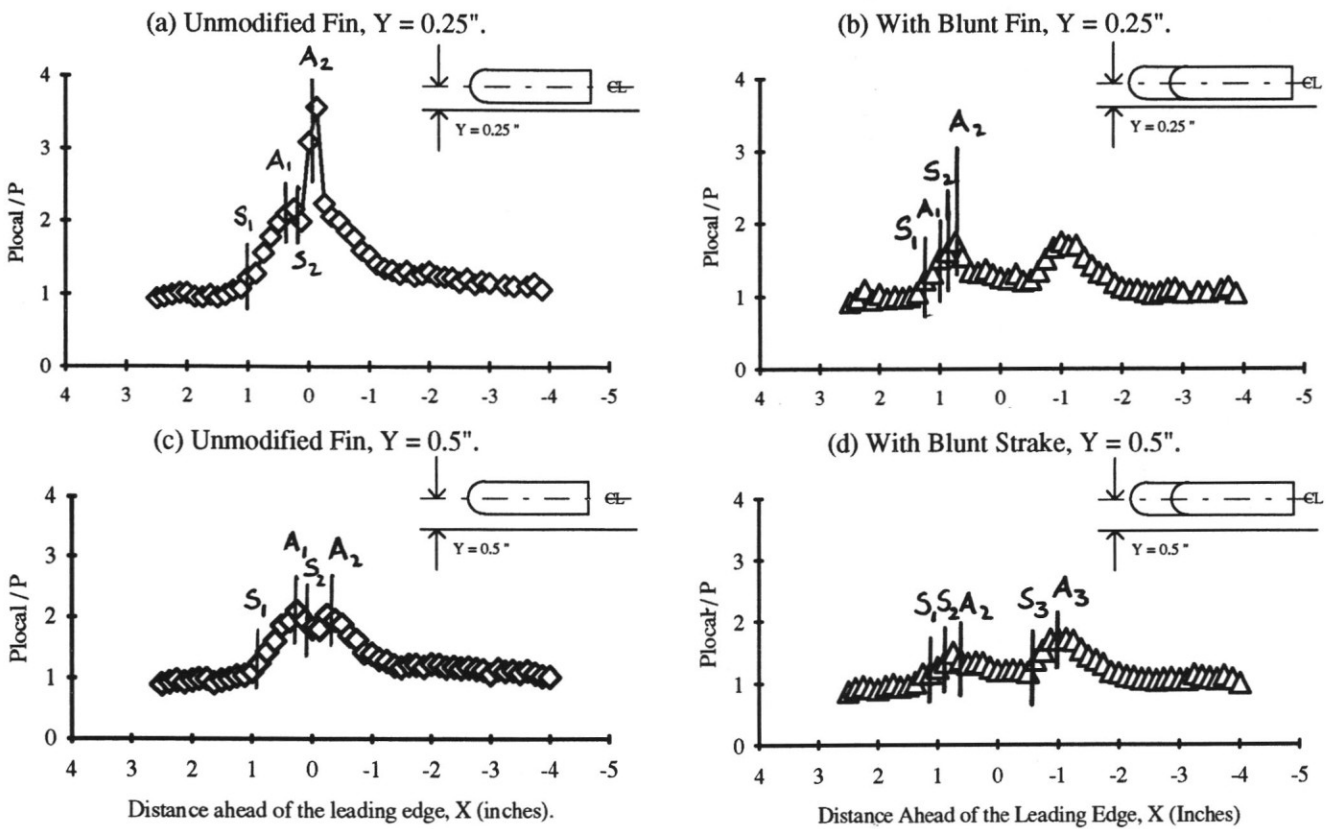
Fig. 5. Oil Flow Photographs for the Model of  $D/\delta=0.6$  With and Without a Blunt Strake.



**Fig. 6. Schlieren Photographs of the Model of  $D/\delta=0.6$  With and Without a Blunt Strake**



**Fig. 7. Pressure Plots for the Fin of  $D/\delta$  With and Without a Blunt Strake.**





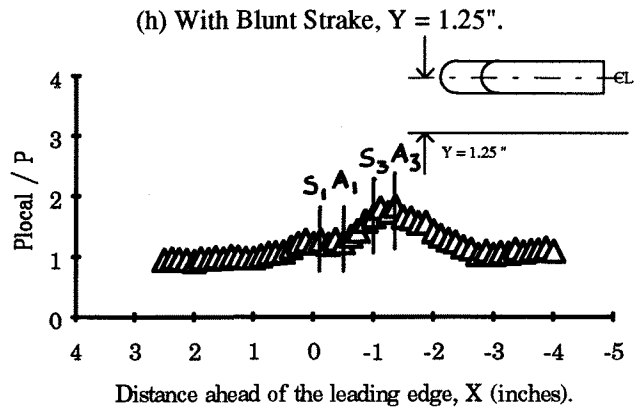
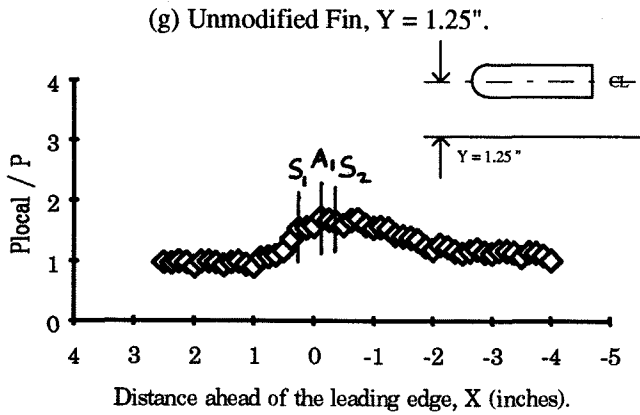
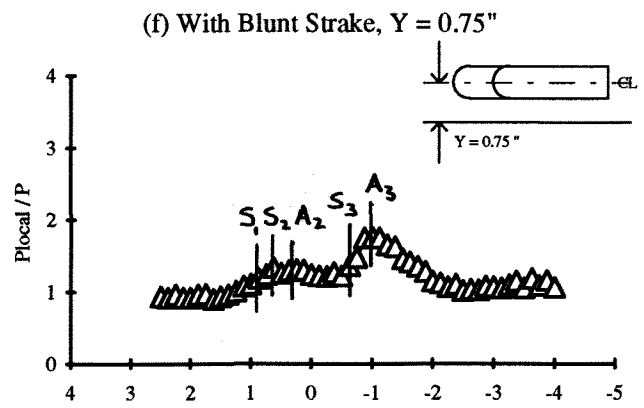
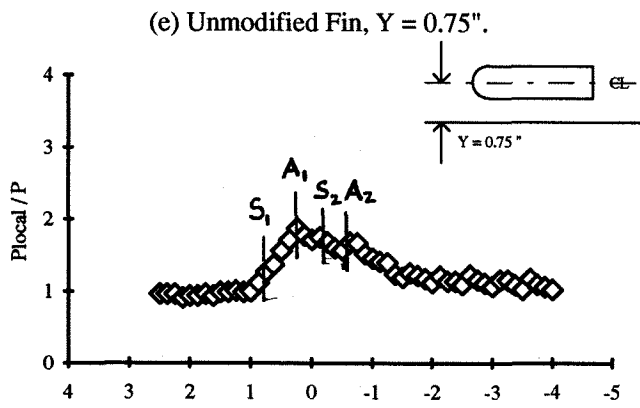
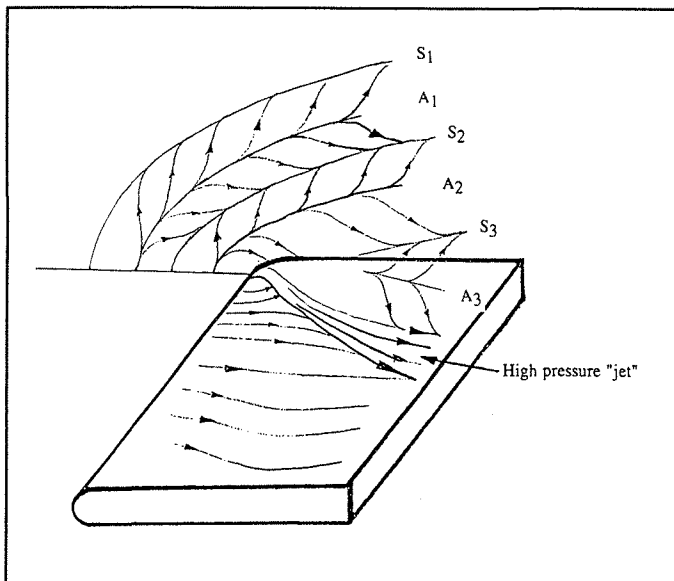


Fig. 8. Flow Field Models for the  $D/\delta=0.6$  Fin with and Without a Blunt Strake.

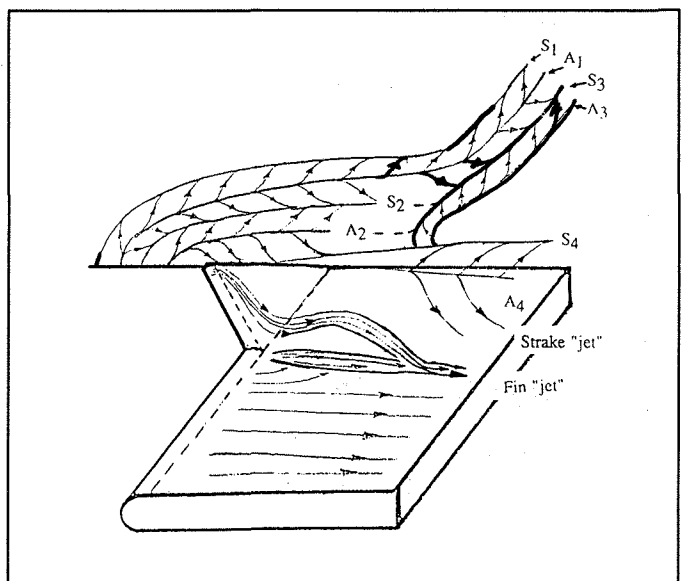
(a) Unmodified Fin

Streak line pattern

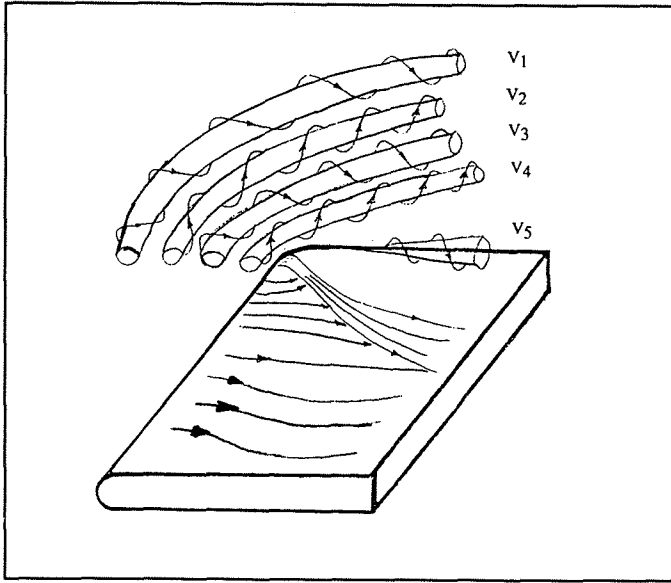


(b) Fin with Blunt Strake

Streak line pattern



Vortex skeleton pattern



Vortex skeleton pattern

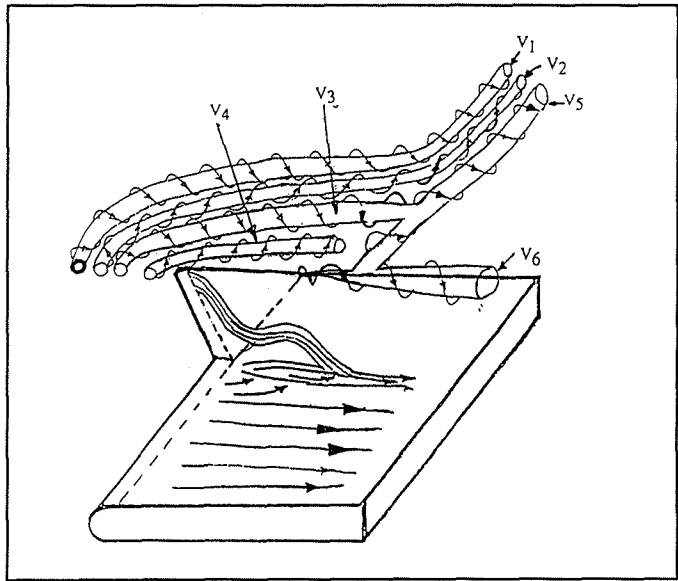
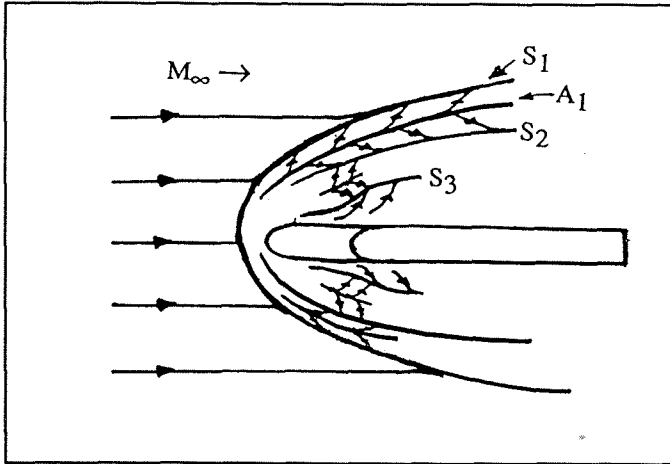
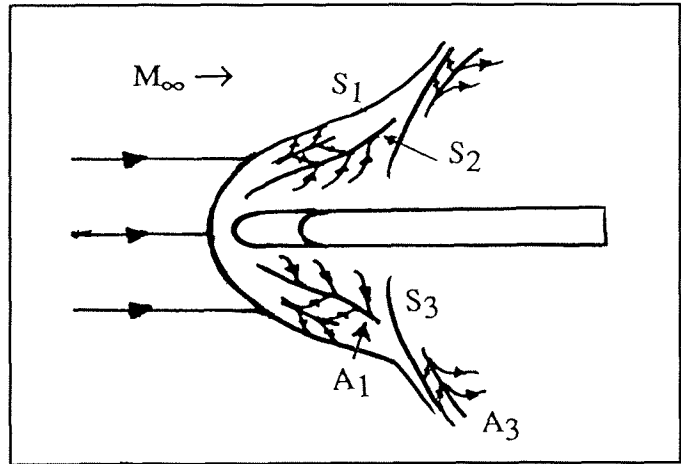


Fig. 9. Sketches of the Oil Flow Photographs for the Models of  $D/\delta=0.682$ .

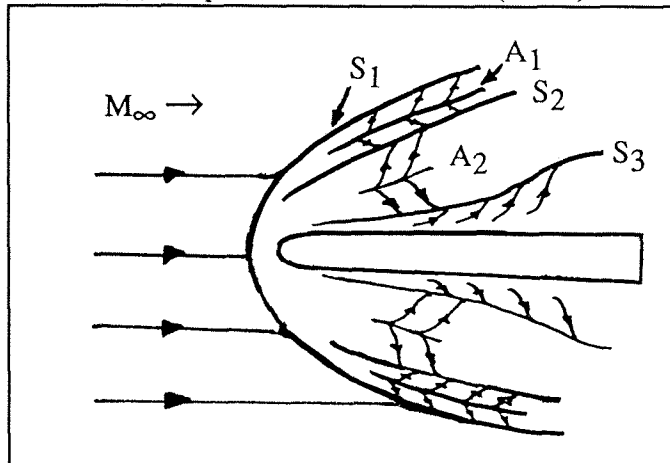
(a) Independent Strake of  $h/\delta=1.6$  (Case 5)



(b) Case 5 Attached to a Straight Fin



(c) Independent Strake of  $h/\delta=3.2$  (Case 7)



(d) Case 7 Attached to a Straight Fin

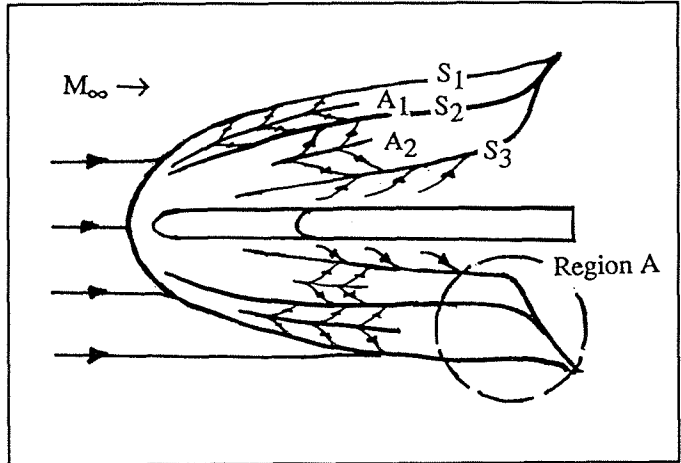


Fig. 10. Sketch Illustrating the Propagation Angle.

